Anomalous behavior of forward I-V and C-V characteristics of Schottky gate AlGaN/GaN HEMTs

M. MOSTEFAOUI[a,*], H. MAZARI[a], K. AMEUR[a], S. MANSOURI[a], N. BENSEDDIK[a], Z. BENAMARA[a], R. KHELIFI[a], N. BENYAHYA[a], J. M. BLUET[b], C. BRU-CHEVALLIER[b], W. CHIKHAOUI[b]

[a]Laboratoire de Microélectronique Appliquée, Département d'électronique, Université Djillali Liabès de Sidi Bel-Abbes, 22000 Sidi Bel-Abbes, Algérie
[b]Institut de Nanotechnologie de Lyon, INL-UMR5270, CNRS, INSA de Lyon, Villeurbanne F-69621, France

In this work we investigate AlGaN/GaN HEMTs structures grown by Low Pressure Metal Organic Chemical Vapour Deposition on SiC substrate. The aim of our work is to study anomalous behavior of the performance results of the characteristics I-V and C-V of (Mo/Au)-AlGaN/GaN HEMTs structure at room temperature. The experimental data were analyzed considering different current-transport mechanisms, such as thermionic emission, generation-recombination, tunneling and leakage currents. The barrier height (ϕ_{bn}), ideality factor (n) and series resistance (R_s) of (Mo/Au)-AlGaN/GaN HEMTs have been calculated from their experimental forward bias current-voltage-temperature (I-V). The capacitance-voltage (C-V) of (Au/Mo)-AlGaN/GaN HEMTs were investigated at room temperature.

1. Introduction

In recent years, the AlGaN/GaN high electron mobility transistors (HEMTs) are excellent candidates for high power electronics and high temperature applications, due to its wide band gap, high thermal stability, and high breakdown voltage [1]. The associated AlGaN/GaN HEMT structure further features relatively high electron mobility due to the existence of the two-dimensional electron gases (2DEGs) [2]. SiC, however, has a higher thermal conductivity (4.9 $W \cdot cm^{-1} K^{-1}$) and presents a smaller lattice mismatch to GaN, therefore it is a more appropriate choice of substrate for high power applications [3]. The Schottky barrier height of the gate electrode is an important parameter for device performance. A large barrier height leads to small leakage currents and higher breakdown voltage which results in the improved noise and power performance of HEMTs [4]. The properties of the semiconductor-metal interface are, in turn, largely dependent on the preparation of the semiconductor surface before metallization [5]. At the metal-semiconductor interfaces, Schottky barrier heights (SBHs) are much more dependent on the metal work function than other III-V materials [6]. Although the SBH depends on the measurement technique, ϕ_{bn}(C-V) is in general greater than ϕ_{bn}(I-V) [7].

This work is an attempt to investigate the anomalous behavior of some Au/Mo/AlGaN/GaN/SiC structure using the I-V and C-V measurements.

An anomalous step was observed in the forward characteristic of the (Mo/Au)-AlGaN/GaN HEMTs. This phenomenon is explained in terms of the presence of two surface phases each having different barrier heights and area [5], and can be mathematically fitted using a simple model called "Two SBH" rectifier in which two Schottky barriers (one high and one low) are connected in parallel [8]. The data obtained were fitted considering various current-transport mechanisms, such as thermionic emission, generation-recombination, tunneling and leakage currents.

2. Experimental details

The layers used in this study were grown by LPMOCVD on SiC substrate. The epitaxial structure is composed of a buffer layer, an undoped 1.2 µm GaN layer and an undoped 25 nm $Al_{0.28}Ga_{0.27}N$ barrier layer. The ohmic contacts are Ti/Al/Ni/Au stacks deposited by evaporation followed by an annealing at 900°C for 30 s under nitrogen atmosphere. Mushroom-shaped Mo/Au gate contacts with Lg = 30 µm gate-length were fabricated using electron-beam lithography. Schematic diagram of AlGaN/GaN HEMTs is shown in Fig. 1. (a) and (b).

The devices are passivated with SiO2/SiN (50/100 nm) using plasma enhanced chemical-vapor deposition (PECVD). After passivation opening, the thick interconnection Ti/Pt/Au metallization is evaporated.
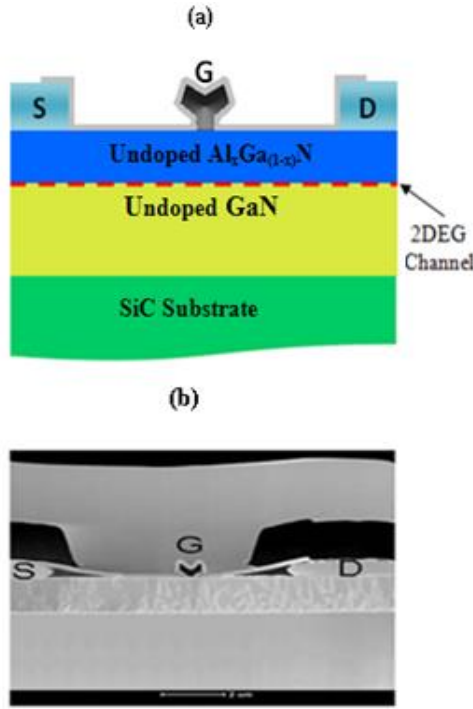
Fig. 1. (a): Schematic of AlGaN/GaN HEMTs
(b): AFM images of HEMTs.

The current-voltage (I-V) measurements were performed by the use of a HP4155B semiconductor parameter analyzer and the capacitance voltage (C-V) measurements were performed at 1 MHz by using a KEITHLEY test system 590 CV Analyser.

3. Experimental results and discussion

3.1. Current-voltage characteristics

We analyze the experimental I-V characteristics by the forward bias thermionic emission theory given as follows [9]:

$$I = I_{TE0} \left\{ \exp\left(\frac{q(V - R_s I)}{nkT}\right) - 1 \right\} \qquad (1)$$

$$I_{TE0} = SA^* T^2 \exp(-\chi^{0.5}\delta) \exp\left(-\frac{q\phi_{bn}}{kT}\right) \qquad (2)$$

Where I_{TE0} is the saturation value of the thermionic current, R_s is the series resistance, S is the device area, q is the electron charge, T the temperature, A^* is the effective Richardson constant ($120\,m_n^*/m_0$ A cm^{-2} K^{-2}), m_n^* is the effective mass of the electron; m_0 is the free electron mass; δ is the interfacial layer thickness, χ is the mean barrier height presented by the thin interfacial layer, k is the Boltzmann constant, and the effective barrier height ϕ_{bn} is given by:

$$\phi_{bn} = \frac{KT}{q} \ln\left(\frac{SA^* T^2}{I_{TE0}}\right) \qquad (3)$$

The ideality factor n is calculated from the slope of the linear region of the forward-bias I-V plot and can be written, from equation (1), as [10]:

$$n = \frac{q}{KT}\left(\frac{dV}{d\ln I}\right) \qquad (4)$$

The currents existing in the structure can be described in general, as a contribution of the following mechanisms: thermionic emission (I_{TE}), the generation-recombination (I_{GR}), tunneling (I_{TU}) and leakage current (I_{LK}). Thus, the total current can be expressed as:

$$I_{tot} = I_{TE} + I_{GR} + I_{TU} + I_{LK} \qquad (5)$$

$$I_{tot} = I_{TE0} \left\{ \exp\left(\frac{q(V - R_s I)}{kT}\right) - 1 \right\}$$

$$+ I_{GR0} \left\{ \exp\left(\frac{q(V - R_s I)}{2kT}\right) - 1 \right\}$$

$$+ I_{TU0} \left\{ \exp\left(\frac{q(V - R_s I)}{E_0}\right) - 1 \right\}$$

$$+ \frac{V - R_s I}{R_p} \qquad (6)$$

Where I_{TE0}, I_{GR0} and I_{TU0} are the particular components at zero bias, E_0 is a parameter dependent on barrier transparency. As suggested by Padovani and Strattson [11]:

$$E_0 = E_{00}\coth\left(\frac{E_{00}}{kT}\right) \qquad (7)$$

$$\text{With} \quad E_{00} = \frac{qh}{4\pi}\sqrt{\frac{N_D}{\varepsilon_s m_n^*}} \qquad (8)$$

ε_s is the permittivity of the semiconductor ($\varepsilon_s = \varepsilon_0\,\varepsilon_r$). ε_0 is the free-space dielectric constant and ε_r is the relative dielectric constant of barrier.

Finally, the leakage component of the current is given by:

$$L_{LK} = \frac{V - R_s I}{R_p} \qquad (9)$$

R_p is the shunt resistance which represents the inhomogeneities and defects at the metal-semiconductor interface.

The forward bias gates I-V characteristics of (Mo/Au)-AlGaN/GaN HEMTs is shown in Fig. 2 at temperature 300 K. We observe the presence of two slopes, a phenomenon was already observed by Morrison et al. [5] and Defives et al. [8], indicates the presence of two diodes. The first diode D1 (low SBH) has a surface smaller than other diode D2 (high SBH).

The saturation current (I_s), ideality factor (n) and series resistance (R_s) determined from the characteristic are respectively: 1.1×10^{-7} A, 1.57, 800 Ω for low SBH and 4.6×10^{-10} A, 7.34, 72 Ω for high SBH.
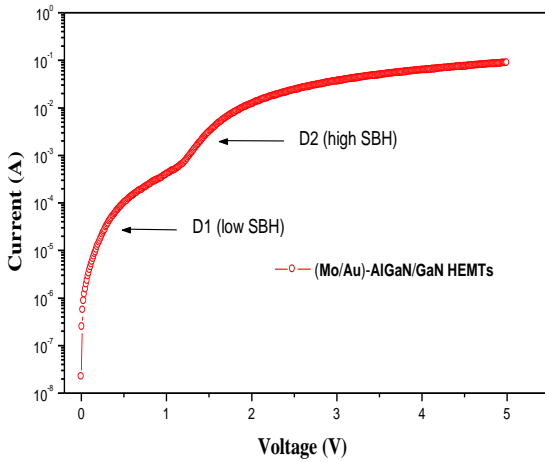
Fig. 2. Experimental forward bias I-V characteristic of (Mo/Au)-AlGaN/GaN HEMTs.

We made an analytical model for the I-V characteristic with different currents. Fig. 3 shows the effect of the thermionic, current, the generation-recombination current, leakage current and the tunneling current on the final relationship.

The parameters chosen for a data fit at 300 K were $I_{TE0} = 10^{-21}$ A, $I_{GR0} = 10^{-12}$ A for $R_s = 72$ Ω, $I_{TU0} = 10^{-7}$ A for $R_s = 800$ Ω, $R_p = 4 \times 10^7$ Ω, $E_0 = 80$ meV. It was noted that the theoretical curve coincides with the experimental curve. The first diode is simulated by a tunneling current with $E_0 = 80$ meV and a leakage current with series resistance $R_s = 800$ Ω and shunt resistance $R_p = 4 \times 10^7$ Ω. The other diode is simulated by a thermionic current$I_{TE0} = 10^{-21}$ A and a generation-recombination current $I_{GR0} = 10^{-12}$ A with series resistance $R_s = 72$ Ω.
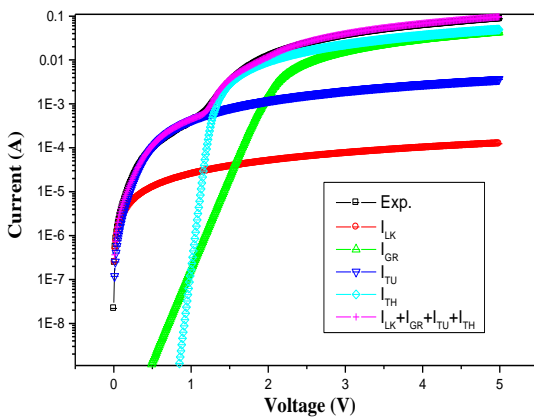
Fig. 3. Experimental and theoretical current-voltage characteristics of (Mo/Au)-AlGaN/GaN HEMTs.

The value of E_0 indicates the presence of a doping concentration $N_D = 3.9 \times 10^{19}$ cm^{-3} this value is very high that the value of the doping of the AlGaN layer, therefore the tunneling current is assisted by defects.

3.2. Capacitance-voltage characteristics

Fig. 4 shows the C-V measurements at 1 MHz and at room temperature for the (Mo/Au)-AlGaN/GaN HEMTs.

The threshold voltage V_{th} (defined by a linear extrapolation of the capacitance curve versus voltage to zero capacitance) is $V_{th} = -5, 19$ V. The 2DEG sheet carrier density n_{2DEG} is given by:

$$n_s = \int \frac{C_{gaz \, 2D} \, dv}{qS} \quad (V: 0 - V_{th}) \qquad (10)$$

Where q is the electron charge and S is diode area. The value of the density of gas evolved from the curve C-V is of the order of 1.1×10^{13} cm^{-3}.

The presence of an negative slope (0 - 0.5 V) this involves an interface state density of acceptors type at the AlGaN/GaN interface, phenomenon observed by Osvald [11].
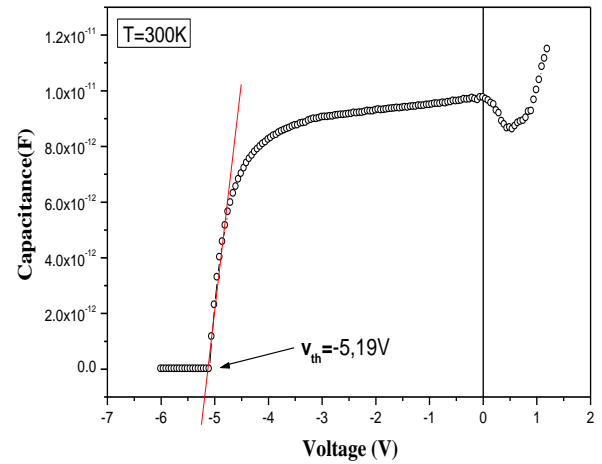
Fig. 4. Experimental C-V characteristics of (Mo/Au)-AlGaN/GaN HEMTs at T = 300 K.

In Fig. 5, the $1/C^2$ data followed with two straight lines. The doping concentration is calculated from the slope in the $1/C^2$ plot using equation (11):

$$\frac{1}{C^2} = \frac{2(V_R + V_0)}{q\varepsilon_s N_D S^2} \qquad (11)$$

Where V_R is the reverse bias voltage, V_0 the diffusion potential, q the electronic charge, S is the surface of the Schottky contact and N_D the doping concentration. In addition, we have determined the net doping concentration N_D and the barrier height ϕ_{bn} from the plot of $1/C^2$ as a function of gate voltage (Fig. 5).We found $N_D = 4.8 \times 10^{17}$ cm^{-3} and $\phi_{bn} = 1.63$ eV (for first slope) and $N_D = 3.09 \times 10^{18}$ cm^{-3} and $\phi_{bn} = 2.7$ eV (for second slope). The AlGaN layer present an first doped layer $N_D = 4.8 \times 10^{17}$ cm^{-3} and an second doped layer $N_D = 3.09 \times 10^{18}$ cm^{-3}.
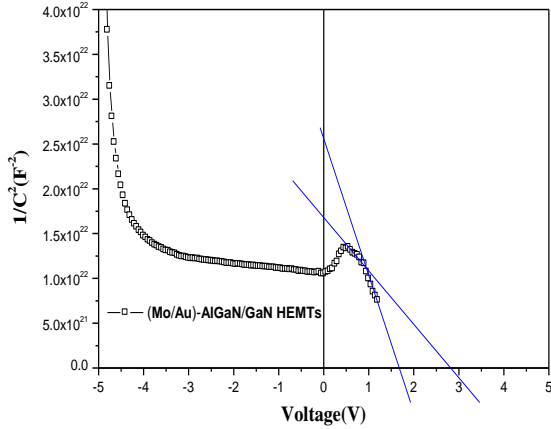
Fig. 5. 1/C^2-V plot of (Mo/Au)-AlGaN/GaN HEMTs.

The carrier concentration profile N_{c-v} are determined by C-V measurements performed at room temperature on the (Mo/Au)-AlGaN/GaN HEMTs. We have deduced the carrier concentration profile N_{c-v} versus the space charge depth W in the heterostructure according to the following relation [12]:

$$N_{C-V} = \frac{c^3}{q\varepsilon_s S^2 (dC/dV)} \qquad (12)$$

and

$$W = S\frac{\varepsilon_s}{C} \qquad (13)$$

Fig. 6 shows the distribution of carrier concentration profile, it exhibits a peak at 36 nm below the surface corresponds to the location of the 2DEG channel formed at the AlGaN/GaN heterostructure [13]. The carrier concentration profile is found to be 3.84×10^{18} cm^{-3}.
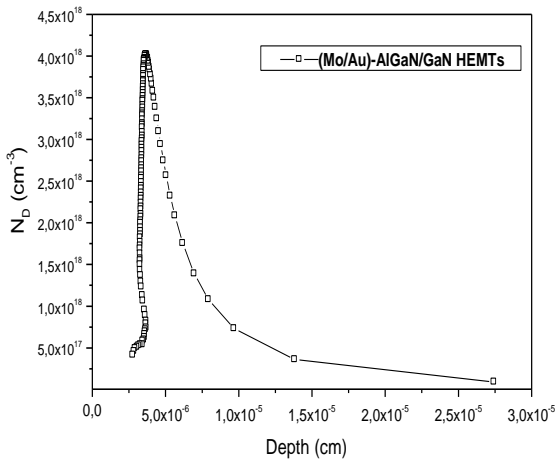
Fig. 6. Profile of the carrier concentration versus the depth W.

3.3. Interface states density characteristics

The density distribution of the interface states N_{ss} in equilibrium with the semiconductor can be determined from the forward bias (I-V) data by taking the voltage dependent ideality factor n(V) and barrier height ϕ_{bn} into

account. The quantities of n(V) can be described as in the following equations, respectively [14]:

$$n = \frac{q}{kT}\left[\frac{(V-IR_s)}{\ln(I/I_s)}\right] \qquad (14)$$

For a diode, the ideality factor n becomes greater than unity as proposed by Card and Rhoderick [15]:

$$n(V) = 1 + \frac{\delta}{\varepsilon_i}\left[\frac{\varepsilon_s}{w} + qN_{ss}\right] \qquad (15)$$

Where ε_i is the permittivity of the interfacial layer, respectively, δ is the thickness of insulator layer, W the width of the space charge region and N_{ss} the density of the interface states. The value of W was calculated from reverse bias C^{-2} vs. V plot as in the following equation:

$$W = \sqrt{\left(\frac{2\varepsilon_s V_d}{qN_d}\right)} \qquad (16)$$

In addition, in n-type semiconductors, the energy of the interface states with respect to the top of the conduction band at the surface of the semiconductor is given by:

$$E_c - E_{ss} = q\left(\phi_{bn} - (V - IR_s)\right) \qquad (17)$$

Fig. 7 shows the energy distribution profile of N_{ss} with and without taking into account R_s obtained from the forward bias I-V characteristics of (Mo/Au)-AlGaN/GaN HEMTs at room temperature. As can be seen in Fig.7, the exponential growth of the interfacial state density is very apparent. The energy values of the density distribution of the N_{ss} are in the range of E_c-0.25 to E_c-0.79 eV.

The magnitude of N_{ss} with and without R_s in E_c-0.25 eV is 2.36×10^{13} eV^{-1} cm^{-2} and 1.38×10^{13} eV^{-1} cm^{-2}, respectively. We observe a peak located at E_c-E_{ss} = 0.28 eV corresponding to a $N_{ss} = 1.98 \times 10^{13}$ eV^{-1}cm^{-2}. So it may indicate the presence of a deep level in this energy [16].

The values of N_{ss} obtained by taking into account the R_s are about one order higher than those obtained without considering the R_s near the conduction band. Therefore the effect of R_s must be taken into account in calculations of main electrical parameters such as n, ϕ_{bn}, and N_{ss} [17].
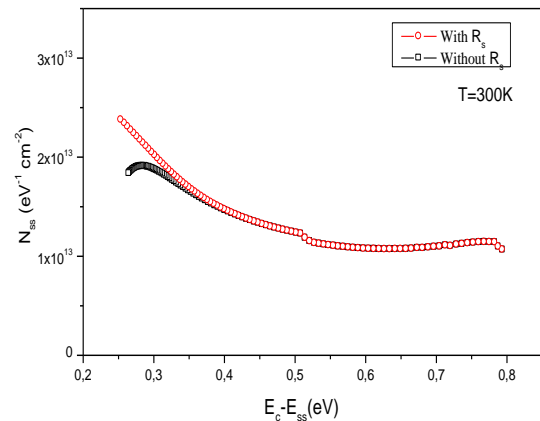
Fig. 7. Energy distribution profiles of N_{ss} as a function of E_c-E_{ss} extracted from the forward bias I-V data of (Mo/Au)-AlGaN/GaN HEMTs at room temperature.

4. Conclusion

The anomalous behavior of the performance results of the characteristics I-V and C-V of (Mo/Au)-AlGaN/GaN HEMTs structures at room temperature are investigated. We noticed the presence of two diodes (one high and one low). Electrical measurements data, from I-V analysis, indicate, in our I-V model, a contribution of the thermionic current, the generation-recombination current, leakage current and the tunneling current. The first diode is simulated by a tunneling current with $E_0 = 80$ meV and a leakage current with series resistance $R_s = 800$ Ω and shunt resistance $R_p = 4 \times 10^7$ Ω. The other diode is simulated by the thermionic current $I_{TE0} = 10^{-21}$ A and the generation-recombination current $I_{GR0} = 10^{-12}$ A with series resistance $R_s = 72$ Ω. From (C-V) experiment curve, we observed an negative slope this involves an interface state density of acceptors type at the AlGaN/GaN interface. The values of N_{ss} obtained by taking into account the R_s are about one order lower than those obtained without considering the R_s. Therefore the effect of R_s must be taken into account in calculations of main electrical parameters such as ϕ_{bn}, n, and N_{ss}. We observe a peak located at $E_c - E_{ss} = 0.28$ eV corresponding to an $N_{ss} = 1.98 \times 10^{13}$ eV^{-1}cm^{-2}.

References

[1] Y. Chen, Y. Jiang, P. Q. Xu, Z. G. Ma, X. L. Wang, T. He, M. Z. Peng, W. J. Luo, X. Y. Liu, L. Wang, H. Q. Jia, H. Chen .J. Electron. Mater .**41**, 3 (2012).

[2] Che-Yang Chianga Heng-Tung Hsua, Edward Yi Changb Physics Procedia **25**, 86-91 (2012).

[3] N. Benseddik. Z. Benamara. H. Mazari, K. Ameur, A. Soltani, J. M. Bluet. Sensor Letters **9**, 2302 (2011).

[4] V. Kumar, D. Selvanathan, A. Kuliev, S. Kim, J. Flynn, I. Adesida Electronics letters **39**, 9 (2003).

[5] D. J. Morrison, K. P. Hilton, M. J. Uren, N. G. Wright, C. M. Johnson, A. G. O'Neill, Materials Science and Engineering B61-**62**, 345 (1999).

[6] Z. Tekeli, Ş. Altındal, M. Çakmak, S. Özçelik journal of applied physics **102**, 054510 (2007).

[7] B Abay, G Çankaya, H. S. Güder1, H. Efeoglu, Y. K. Yogurtçu, Semicond. Sci. Technol. **18**, 75 (2003).

[8] D. Defives, O. Noblanc, C. Dua, C. Brylinski, M. Barthula, V. Aubry-Fortuna, and F. Meyer, IEEE Trans. Electron Devices **46**, 449 (1999).

[9] E. H. Rhoderick, R. H. Williams, Metal-Semiconductor Contacts,Clarendon Press, Oxford (1988).

[10] Engin Arslan, Emsettin Altındal, Uleyman Ozc, Elik Ekmel Ozbay. Semicond. Sci. Technol. **24**, 6 (2009).

[11] J. Osvald, IEEE. **7,** 167 (2010).

[12] Manel Charfeddine, Malek Gassoumi, Hana Mosbahi, Christophe Gaquiére, Mohamed Ali Zaidi, Hassen Maaref, Journal of Mod Phys. **2**, 1231 (2011).

[13] M. Gassoumi, S. Saadaoui, M. M. Ben Salem, C. Gaquiere, H. Maaref, Eur. Phys. J. Appl. Phys. **55**, 3 (2011).

[14] H. C. Card, E. H. Rhoderick, J. Phys. D: Appl. Phys. **4**, 1589 (1971).

[15] S. Altındal, H. Kanbur, A. Tataroglu, M. M. Bülbül, Physica B: Condensed Matter. **399**, 146 (2007).

[16] W. Chikhaoui, J. M. Bluet, P. Girard, G. Bremond, C. Bru-Chevallier, C. Dua, R. Aubry, Physica B: Condensed Matter, **404**, 4877 (2009).

[17] İlke Taşçıoğlu, Umut Aydemir, Şemsettin Altındal, Barış Kınacı, Süleyman Özçelik, J. Appl. Phys. **109**, (2011).

_____

*Corresponding authors: mohamedmicro82@gmail.com
                        h_mazari2005@yahoo.fr